

Short Circuit Faults Identification and Localization in IEEE 34 Nodes Distribution Feeder Based on the Theory of Wavelets

Sara J. Authafa

College of Engineering/Power and Machines Department, Basra, Iraq

Email: saraauthafa7@gmail.com

Khalid M. Abdul-Hassan

College of Engineering/Power and Machines Department, Basra, Iraq

Email: khhmh7447@gmail.com

Abstract—In this paper a radial distribution feeder protection scheme against short circuit faults is introduced. It is based on utilizing the substation measured current signals in detecting faults and obtaining useful information about their types and locations. In order to facilitate important measurement signals features extraction such that better diagnosis of faults can be achieved, the discrete wavelet transform is exploited. The captured features are then utilized in detecting, identifying the faulted phases (fault type), and fault location. In case of a fault occurrence, the detection scheme will make a decision to trip out a circuit breaker residing at the feeder mains. This decision is made based on a criteria that is set to distinguish between the various system states in a reliable and accurate manner. After that, the fault type and location are predicted making use of the cascade forward neural networks learning and generalization capabilities. Useful information about the fault location can be obtained provided that the fault distance from source, as well as whether it resides on the main feeder or on one of the laterals can be predicted. By testing the functionality of the proposed scheme, it is found that the detection of faults is done fastly and reliably from the view point of power system protection relaying requirements. It also proves to overcome the complexities provided by the feeder structure to the accuracy of the identification process of fault types and locations. All the simulations and analysis are performed utilizing MATLAB R2016b version software package.

Index Terms—distribution feeder, wavelets, fault detection, fault classification, fault location, cascade forward neural networks, IEEE 34 test feeder.

I. INTRODUCTION

Owing to the exposure to natural environment, the overhead distribution feeders are prone to external fault causes including rain, wind, lightning and interference with objects like trees and vehicles. Fault causes can also be internal such as insulation degradation and failure. The formation of a conducting path between phase conductors and ground or between one phase conductor and another, will usually cause the flow of high amounts of short circuit currents. Consequently, a risk may be imposed on humans and power system equipments if the isolation process was slow or absent. This has led to the proposal of many fault identification techniques in an effort to reduce fault risk circumstances. The use of wavelet analysis introduces a powerful tool to extract important fault signatures and facilitate fault diagnosis. The results are fast response, cost effectiveness and accuracy. A lot of the researches work made use of the discrete wavelet transform (DWT) at high stages, wherein, the fault signatures can be more significant such that more

accuracy can be obtained. However, the choice of the most suitable stage is dependent on the application, on the chosen mother wavelet, on the sampling frequency, and on the length of the signal to be analysed. The large number of decompositions, filter length and the nature of the extracted feature can impose more processing time which is non preferable for the detection of faults process [1]. As a result, building a scheme for which good accuracy of decisions, as well as fast responsiveness is desirable in the field of protection relaying. The reviewed techniques are based mostly on studies of the detection, classification, and localization of faults or a combination between the three schemes. References [2]-[3] presented a study of the detection of faults, whereas [4]-[6] presented the classification of faults. A combination between the detection and classification of faults is introduced in [7]-[9]. These techniques are dependent mostly on the artificial intelligence. A number of fault localization schemes are introduced in [10]-[19]. Out of these schemes, Four methods of faults localization can be recognized. They can be based on the travelling wave equation application as in [10]-[11], or on calculating the

apparent impedance up to the point of fault as in [12]-[13], on a ranking analysis according to a previously stored database as given by [14]-[15], or on the artificial intelligence applications as can be seen in [16]-[19]. An overall protection scheme that utilizes the artificial neural networks (ANNs) in building the detection, type recognition and localization of faults is presented in [20]-[21].

It can be seen from the literature survey that some of the techniques are dedicated for the protection of transmission lines, others are dedicated for protection of the distribution feeders. The techniques applicable to the protection of transmission lines may be inaccurate for the protection of distribution feeders. This is due to the usual complexity in distribution feeders structure provided by the non-homogeneity of feeder lines (the difference in impedances between the different line sections) and the presence of laterals and load branches [16][22]. In the last few years, the advancements in signal processing and artificial intelligence techniques are utilized in the field of power systems digital protection relaying. The less complexity in fault diagnosis approaches, the improved accuracy in the decisions and predictions made, as well as the fast responsiveness provided a superiority over the old protection relaying techniques [23].

In this paper, a standard distribution feeder system having the characteristics of being long, lightly loaded, non-homogeneous, and branched with a number of laterals is built and simulated. Measurement current signals obtained at the substation are collected and analysed with the help of the discrete wavelet transform (DWT). Based on the various signals DWT extracted features variations with faulty and healthy feeder states, as well as with fault types and locations, a protection scheme is built and tested. The proposed protection scheme is built based on three stages. The first stage is the detection of faults scheme that is based on utilizing a specific function characteristics to facilitate faster and accurate faults occurrence or absence diagnosis. With the help of the moving frame technique [24], further improvement in the speed of faults detection can be obtained. The second stage of the protection scheme is based on the classification of shunt faults ten types, i.e. finding the faulted phases involved. The third stage is the localization of faults scheme that indicate the distance of faults from the main substation in meters. In addition to providing an information of whether the faults are localized at the main feeder or on one of the laterals. The fault type and localization schemes are built based on a specific type of neural networks called the cascade forward neural nets (CFNN). Such neural networks prove to have the capability to capture the complex relationship between the signals extracted features with fault type once and location secondly.

II. A GENERAL OVERVIEW OF WAVELET ANALYSIS

In power system fault analysis, it is important to detect certain trends in the signals to be analysed to improve the

detection process. Wavelet transform (WT) analysis have proven to be the best choice for fault identification techniques; wherein, a variable windowing technique is utilized to analyse non-stationary signals (having localized changes which is the dominant behaviour of faulty signals). In this technique, accuracies in both time and frequency can be gained as compared to discrete Fourier transform (DFT) that has one fixed resolution in time and frequency which is regarded as a drawback. The major advantage of the WT is its capability in revealing aspects like trends, breakdown points and discontinuities. The basis function used by wavelet analysis is called wavelets which they are waveforms of finite duration with irregularity trends and an average value of zero. There are several types of Wavelet transform that originated from a basic one called continuous wavelet transform (CWT). The CWT is defined as the sum over all time of the analysed signal multiplied by shifted and scaled versions of the basis function (mother wavelet function Ψ) as following:

$$\Psi(a, b) = a^{-1/2} \Psi(a^{-1}(t-b)) \quad (1)$$

$$C(a, b) = \int_{-\infty}^{+\infty} f(t) a^{-1/2} \Psi(a^{-1}(t-b)) dt \quad (2)$$

Where, C: the wavelet coefficient that represents how closely the wavelet is correlated with that part of the signal $f(t)$. a : scaling parameter, b : shifting parameter.

Since Any signal processing method performed in a computer using real world data must be accomplished in a discrete state, and since calculating CWT provides redundancy of values because of the small shifting and dilating steps, the choice of a finite number of scale and position steps based on a power of 2 (dyadic steps) has been introduced as following :

$$a = 2^j, b = \mu 2^j \quad (3)$$

$$W(j, \mu) = \sum_k f(k) 2^{-j/2} \Psi(2^{-j}k - \mu) \quad (4)$$

Where, $W(j, \mu)$: the DWT coefficients as a function of the new scaling and shifting parameters j and μ .

This approach is called the discrete wavelet transform (DWT) that can be realized using a set of filters into which the signal is passed and out of which the coefficients are emerged. Multi Resolution Analysis (MRA) is the iterative process of decomposing the analysed signal by the DWT filters into approximation and detail components. Approximations represent low frequency components of the signal whereas details represent high frequency components. The signal that enters the DWT filters will be decomposed according to the MRA as shown in Fig. 1. Where, cA : is the approximation coefficients, cD : detail coefficients, $h(k)$ and $g(k)$: the low and high pass filters coefficients respectively.

It can be seen through the figure that the signal after being convolved with the filters transfer functions, is down sampled by 2 in order to avoid duplication of the samples at each stage. The result is equal amount of samples as that of input signal.

The frequency division of a signal by the MRA analysis is shown in Fig. 2, where f_s : is the sampling frequency that satisfies Nyquist's sampling criteria. The first decomposition stage will divide the signal in the frequency domain into two halves. The second stage will decompose the first stage approximations frequency range into other two halves and so on.

The DWT is chosen in this work to analyse the current signals due its superiority as a pre-processing tool that can capture the useful signals aspects and reduce the needs to the unnecessary redundant data. Besides it is widely used in the field of power systems protection relaying for the detection, type classification, or localization of faults in both transmission and distribution systems as can be seen in the reviewed literature.

In order to perform fault test cases, a standard distribution feeder of an overhead radial type is built with MATLAB SimPowerSystems toolbox. The model is chosen to be the IEEE 34 node test feeder which is a long, lightly loaded feeder with many laterals. The original model specifications are given in [25], the modelled feeder in this paper is scaled down to the 11 kV system instead of 24.9 KV system keeping the current value the same. The line series impedances and load power ratings are multiplied by a factor ($k = 11/24.9 = 0.4418$) and the shunt capacitance values are divided by the same factor, the scaling method is provided in [26]. The topology of the feeder is shown in Fig. 3. For accurate representation of feeder conductors impedances, the pi section block is used. The loads are modelled as given in [25], [27].

III. DISTRIBUTION FEEDER MODEL

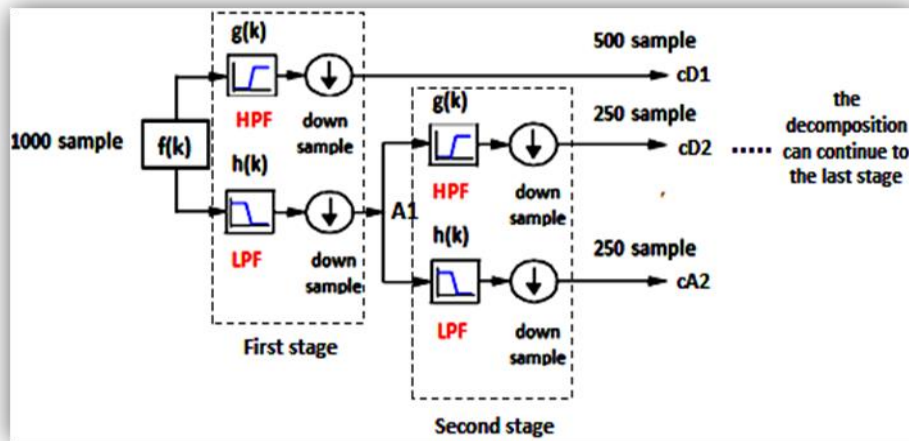


Figure 1. DWT MRA analysis

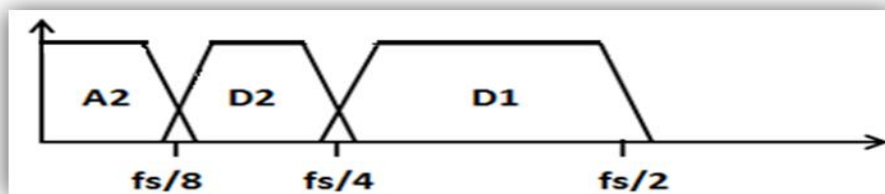


Figure 2. Frequency band division by the DWT

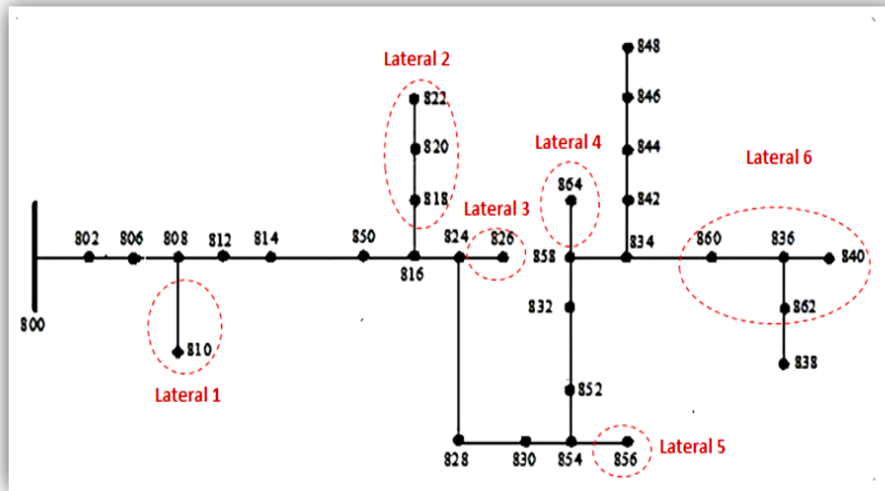


Figure 3. Feeder Topology

IV. THE SIGNAL PROCESSING REQUIREMENTS FOR THE PROPOSED SCHEME

In order to build a fast and reliable protection scheme, the following considerations must to be taken into account:

A. Sampling Frequency

In order to correctly represent any signal in the discrete state, the sampling frequency (f_s) has to be equal to or larger than double the highest frequency content of the signal. This is how the successful sampling of signals is governed by the Nyquist's sampling criteria. The range of frequencies contained in faulty power system transient signals usually lies between 0.1-1000 Hz [28]. Therefore, (f_s) has to be chosen such that it can be larger than or equal to 2 kHz. Consequently, the measurement signals in this work are sampled at an (f_s) of 6.4 kHz, which means having a simulation sampling time (T_s) of 1.563e-4 seconds. The value of (f_s) is calculated based on the following:

The number of samples per cycle has to be chosen firstly based on a power of two as required by the DWT of signals. In this work, the chosen number of samples per cycle is 128. This choice provides the enough accuracy required by the protection scheme stages as will be shown later in the test results. Multiplying 128 samples/cycle by the fundamental frequency of signals (50 Hz) will provide the mentioned (f_s) [29].

B. The Suitable Mother Wavelet Test

The accuracy of the wavelet transform analysis can be greatly affected by the choice of the mother wavelet. A number of tests exists for the purpose of choosing the best mother wavelet for the analysis of specific type of signals. Since the WT coefficients values represent a measure of how the analysed signal is similar to the analysing mother wavelet, having the analysed signal important aspects condensed within a few number of coefficients can define the effectiveness of the analysing mother wavelet. This is how the maximum energy to Shannon entropy (MESE) criteria can identify the

suitability of the mother wavelet function for a specific analysis [30][31]. MESE is chosen to be the criteria to test for the suitable mother wavelets dedicated for the analysis in this work. It is calculated as given in (5), where the energy content of coefficients can be calculated according to Parseval's formula as given in (6), and the normalized Shannon entropy is calculated as given in (7).

$$MESE = \frac{\sum_{j=1}^M E_j}{\sum_{j=1}^M S_j} \quad (5)$$

$$E_j = \sum_{k=1}^N |c_{jk}|^2 \quad (6)$$

$$S_j = - \sum_{k=1}^N \frac{|c_{jk}|^2}{E_j} \cdot \log_2 \left(\frac{|c_{jk}|^2}{E_j} \right) \quad (7)$$

Where, E_j : is Parseval's energy of coefficients related to a specific analysis resolution (j), S_j : is the Shannon entropy of coefficients related to the resolution (j). M : is the total number of analysis resolutions. c_{jk} : is the individual WT coefficient that related to the resolution (j) and of a sequence (k). N : is the total number of coefficients at the resolution (j).

The MESE is performed in this work as follows:

- Two sets of measurement signals of a length of 8 cycles (having 1024 samples) are collected, one to test the most suitable mother wavelet for the detection scheme, and the other to perform the test for the type and location schemes. The total number of signals collected for the detection scheme is 9 signals that involve the healthy state, as well as the faulty and non-faulty transient states (like capacitor and feeder energization events). On the other hand, the total number of signals collected for the type and location schemes is 50 signals that result from simulating faults at 5 different locations on the feeder involving the 10 types of faults.
- Each signal will be decomposed up to the 7th level to get 14 resolutions (7 approximations and 7 details) by a set of test mother wavelets.

- E_j and S_j will be calculated for each resolution according to (6) & (7) respectively.
- MESE will be calculated as given in (5), where the obtained E_j and S_j will be summed for all resolutions and the ratio between them will be obtained.
- The average of the MESE of the set of signals will be calculated to obtain one value specific to each tested mother wavelet.
- The above steps will be repeated for each test mother wavelet.

The test results are shown in Table I for the detection scheme signals analysis, and in Table II for the fault type and localization schemes signals analysis. The best mother wavelet is the one that have the maximum MESE.

TABLE I. THE TEST RESULTS OF THE MESE FOR THE DETECTION SCHEME SIGNALS ANALYSIS

Mother Wavelet	MESE Measure
Db1	1.1742e+6
Db2	2.0131e+6
Db3	1.7977e+6
Db4	1.9608e+6
Db5	1.9401e+6
Sym1	1.1742e+6
Sym2	2.0131e+6
Sym3	1.7977e+6
Sym4	1.9423e+6
Sym5	1.9051e+6
Coif1	1.8022e+6
Coif2	1.9399e+6
Bior 1.1	1.1742e+6
Bior 1.3	1.6083e+6

TABLE II. TEST RESULTS FOR THE MESE OF THE FAULT TYPE AND LOCALIZATION SCHEMES SIGNALS ANALYSIS

Mother Wavelet	MESE Measure
Db1	2.5556e+7
Db2	3.787e+7
Db3	4.1205e+7
Db4	4.3197e+7
Db5	3.6666e+7
Sym1	2.5556e+7
Sym2	3.787e+7
Sym3	4.1205e+7
Sym4	4.2612e+7
Sym5	3.245e+7
Coif1	3.462e+7
Coif3	4.2316e+7
Bior 1.1	2.5556e+7
Bior 1.3	3.7266e+7

It can be seen that the best mother wavelet that has the maximum value of MESE is the Db2 for the detection of faults scheme signals analysis, and the Db4 for the fault type classification and localization schemes signals analysis.

C. Frame Size:

The window length at which the current signals will be analysed is chosen to be of 128 samples, i.e. of a length of one cycle. This choice is made based on many tests regarding the accuracy of the built protection schemes.

D. Framing Technique

Since the current samples must be processed in frames, the framing method can increase or decrease the processing speed. The moving frame method is implemented in this work to keep the detection speed as fast as possible [24]. This method is based on entering one sample at a time to the analysis window (the frame) at the same time of leaving one sample behind. The resultant is the least amount of delay time as compared to the original framing method that requires for the whole frame to be collected for processing. Figs. 4 & 5 represent the original framing technique and the moving frame techniques respectively. Figs. 6 & 7 show the high improvement of detection speed by the application of the moving frame technique.

E. The Number of Decomposition Stages

The highest number of decomposition stages depends on the length of the analysed signal as given in (8):

$$D = \log_2 (L) \quad (8)$$

Where, D: the highest number of decomposition stages, L: the length of the analysed signal.

Reducing the number of decomposition stages will provide a reduction in the number of convolutions and down sampling processes performed within the DWT. As a result, the processing time will be reduced and the detection of faults will be faster. Therefore, the detection scheme is built based on the first analysis stage. This choice provides the required accuracy and reduction in computational burden. As regard to the fault type and location identification schemes, a three stages of DWT decompositions are found to yield the best accuracy in the predictions of such schemes.

F. Features Representation

In order to introduce the DWT coefficients as a measure of the various feeder system states, there must be a certain representation of their variations. In this work, Parseval's formula that calculates the energy of coefficients presented at a specific resolution as given in (6) is utilized.

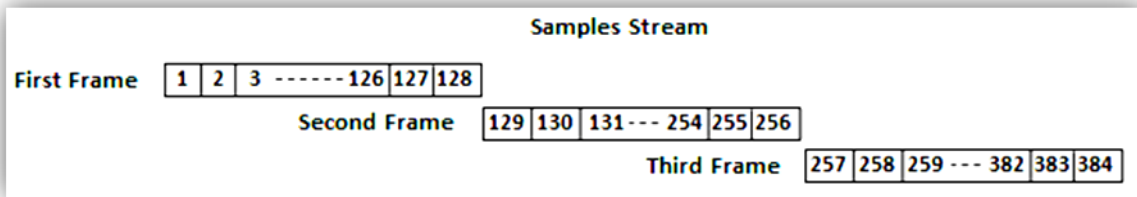


Figure 4. The original framing technique

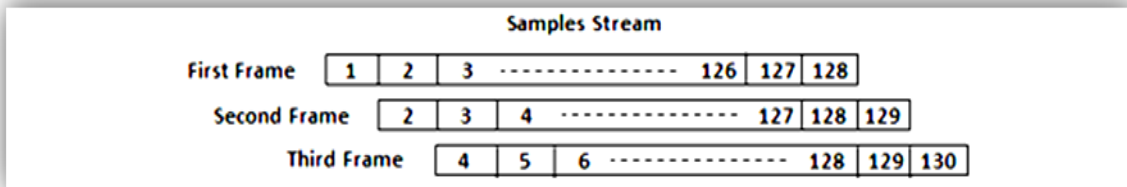


Figure 5. The moving frame technique

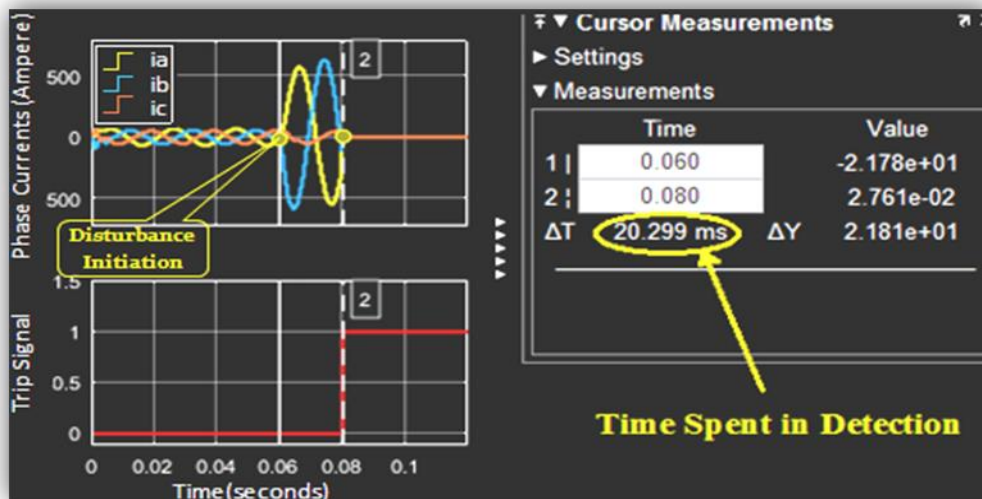


Figure 6. Faults detection and tripping after utilizing the old framing technique

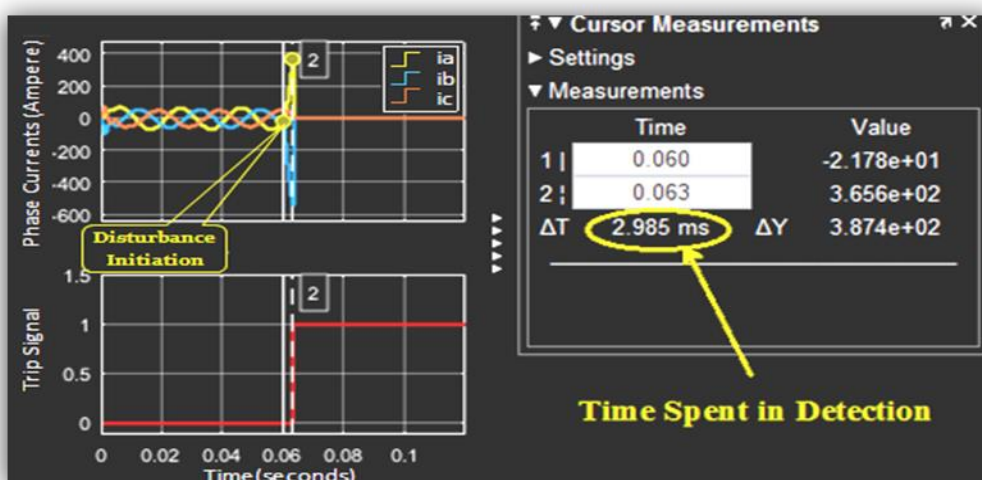


Figure 7. Faults detection and tripping after utilizing the moving frame technique

V. THE PROPOSED PROTECTION SCHEME

The proposed fault protection scheme is based onto three stages:

A. The Fault Detection Stage

The requirement of a fast and reliable detection scheme has led to the utilization of a function provided in [1]. Where the phase currents are root squared summed to form one waveform that concentrate the fault transients and facilitate faster detection of faults. The function formula is given in (9):

$$f[n] = (I_a[n]^2 + I_b[n]^2 + I_c[n]^2)^{1/2} \quad (9)$$

The provision of some healthy feeder state transient events such as those caused by the energization of the feeder or a power factor correcting capacitor bank can produce a high frequency components in the measured current signals. These components affect the detail coefficients obtained by the DWT analysis in a manner that it can exceed those related to the faulty states. However, the approximation coefficients will still within the normal limits during the healthy state transient events. On the other hand, the faulty states will cause a rise in both the approximation and detail coefficients of the analysed current signals. A number of feeder states presented in Table III, where $f[n]$ for a one cycle of measurements is analysed by the Db2 related DWT filters for the first stage to reveal the effects of the various healthy and faulty events on the energy of the obtained coefficients. All the presented faulty cases are simulated at node 812 regarding a zero fault resistance. Based on the data presented in the previous table and other data provided by performing many faulty cases tests on various feeder locations regarding various fault types and fault resistances, two thresholds are set to distinguish between healthy and faulty feeder states. These thresholds are based on the values given by:

Threshold1 =4.0425e+6; Threshold2 =8.25

The DWT analysis performed on $f[n]$ to detect faults are provided in Fig. 8. The flow chart for the detection of faults stage is provided in Fig. 9, where the Db2 related DWT first stage approximation and detail coefficients energies $eA1$ and $eD1$ are calculated and compared with the thresholds to diagnose the feeder state.

TABLE III. THE DIFFERENT FEEDER STATES REPRESENTED BY THE ENERGY OF DWT COEFFICIENTS OBTAINED AT THE FIRST STAGE OF $f[n]$ ANALYSIS WITH THE HELP OF DB2

Feeder States	DWT Coefficients	Energy of Coefficients After the Disturbance
Healthy	cA1	5.8828e+05
	cD1	0.1984
Capacitor Energization	cA1	7.3732e+05
	cD1	297.3107
Feeder Energization.	cA1	7.7711e+05
	cD1	779.218
Single Line to Ground Fault at Node 812	cA1	2.4792e+07
	cD1	261.6058
Double Line to Ground Fault at Node 812	cA1	1.1997e+08
	cD1	1.2246e+03

Double Line Fault at Node 812	cA1	1.1494e+08
	cD1	2.3689e+03
Three Line Fault at Node 812	cA1	1.708e+08
	cD1	5.0149e+03

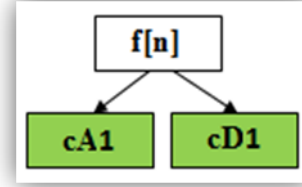


Figure 8. $f(n)$ related DWT first stage analysis with the help of Db2 for the detection of faults scheme

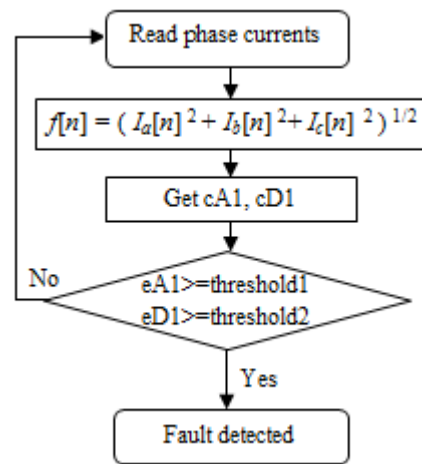


Figure 9. The flowchart for the fault detection procedure

B. The Fault Type and Localization stages

1) Artificial neural Networks Application:

The CFNNs are used to indicate fault type and location. These type of neural networks are a feed forward nets with additional weight connections between layers, adding the connections will provide better learning capabilities as compared to ordinary feed forward nets [32].

To build the network the following considerations must be taken into account [32]:

- Choose the features to be extracted from the current signals and feed it to the ANN.
- The provided data for the network must be divided into training, validation and test sets. A specific neural network toolbox built-in function called divide random is used such that the provided set of simulated fault cases extracted features are divided randomly to 80% training and 20% validation data with an individual set provided to test for the network generalization.
- The inputs will be pre-processed by another built-in functions such as map min-max that transforms input data such that all their values will fall in the interval [-1,1], the other function is remove constant rows that removes duplicated input values. The targets will

have the same processing functions in order to transform the provided targets to useful values for the network use, after that the network outputs will be reverse processed to provide the same user provided output data. The provision of such functions is to improve network learning capabilities.

- Decide the number of neurons and the structure of the hidden layer.
- Train the network by a chosen training function to have the least mean squared error (mse).

Tables IV and V provide faults simulations locations and their distances provided for the ANN training and testing procedures. The faults resistances are taken into account such that the CFNNs are trained regarding fault resistances ranging from 1-50 in steps of 5 ohms. The test sets are provided for fault resistances which are: 3, 7, 21 and 33 ohms.

2) *Fault Type stage:*

After performing a number of tests, the fault type ANN input features are chosen as the energy representation of the first stage approximations, second and third stage details of the db4 decomposed three phase and zero sequence current samples. As a result, the fault

type ANN will have 12 inputs. The inputs of the network are obtained after performing the analysis shown in Fig. 10, where the shaded features are the ones used in the fault type classification procedure. The fault type ANN specifications are given in Table VI.

3) *Fault Localization Stage:*

A modular type ANN [20], consisting of individual ANNs of CFNN type for each type of fault is used for finding fault locations as shown in Fig. 11. For this type of network, there will be an improvement in the learning process and the accuracy of the results as compared to using a network consisting of one block for estimating the location for all fault types. The inputs of the fault location network are the same 12 extracted features provided for the fault type scheme. The fault location ANNs will predict the fault distance from source in meters and their locations if they were on the main feeder or laterals. The flow chart of the fault location process is shown in Fig. 12. The network specifications are shown in Tables VII & VIII respectively.

TABLE IV. THE LOCATIONS AT WHICH FAULT SIMULATIONS ARE PERFORMED IN ORDER TO COLLECT SUBSTATION MEASUREMENT SIGNALS FOR LATER UTILIZATION IN THE TRAINING PROCESS OF FAULT TYPE AND LOCATION NEURAL NETS

Main Location	Distances in (km)													
Main Feeder	0.3474	2	4.92	6	8	12	15.388	15.501	18.282	22	24	24.683	25.353	25.424
Lateral.1	5.702													
Lateral.2	14.243	16	20	21.189	21.419									
Lateral.3	15.796													
Lateral.4	19.137	21.493												
Lateral.5	24.191													
Lateral.6	24.917	25.278	25.979											

TABLE V. THE NODES AT WHICH FAULT SIMULATIONS ARE PERFORMED IN ORDER TO COLLECT SUBSTATION MEASUREMENT SIGNALS FOR LATER UTILIZATION IN THE TESTING PROCESS OF FAULT TYPE AND LOCATION NEURAL NETS

Main Location	Distances in (km)						
Main feeder	4	9.97	13.97	16	20	23.3115	24.8636
Lateral.1	5.1157						
Lateral.2	15.864	18	20.727				
Lateral.3	15.49						
Lateral.4	20						
Lateral.5	24.0273						
Lateral.6	25.4788						

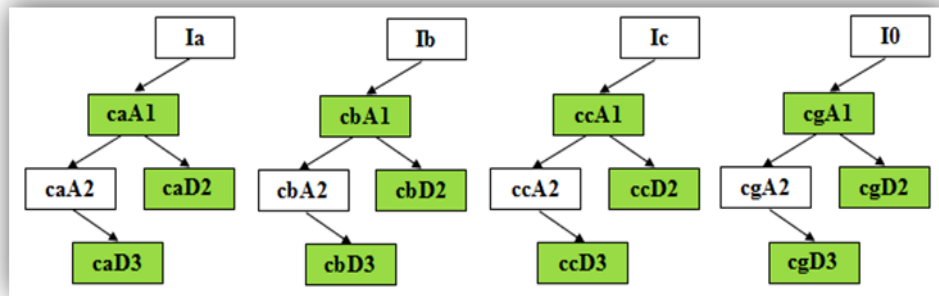


Figure 10. The three phase and zero sequence current signals Db4 related DWT first, second, and third stage analysis coefficients obtained for the utilization in the fault type classification and localization schemes

TABLE VI. FAULT TYPE NEURAL NETWORK SPESIFICATIONS

Type of ANN	Cascade forward net
No. of hidden layer neurons	48
Network structure	12-12-12-12-1
Hidden layer transfer function	Tan Sigmoid
Output layer transfer function	Linear
Performance function	Mean squared error (MSE)
Training function	Trainlm
Training performance	3.4312e-7
Best validation performance	3.99e-7
Test performance	9.2064e-5
Epochs	366

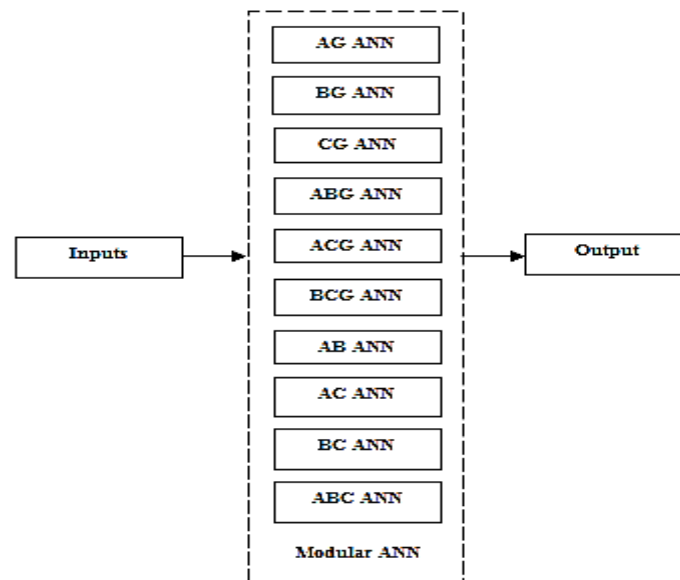


Figure 11. Fault location neural network modular structure

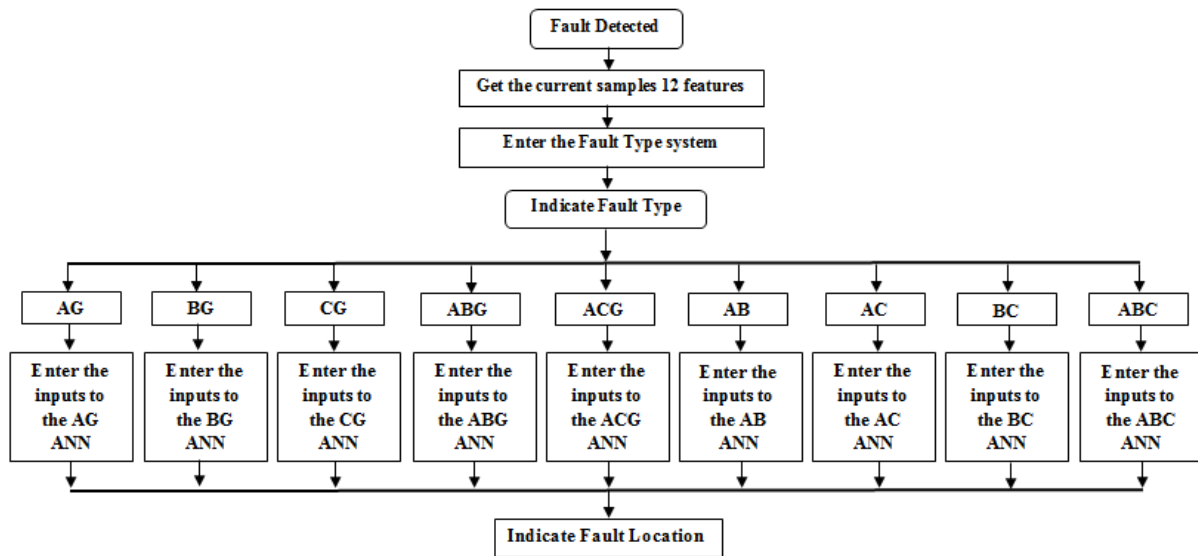


Figure 12. Fault type and location indication flow chart

TABLE VII. DISTANCE PREDICTING FAULT LOCATION NEURAL NETS SPECIFICATIONS

Type of ANNs	Cascade forward net					
Hidden layer transfer function	Tan sigmoid					
Output layer transfer function	Linear					
Training function	Trainlm					
Performance function	Mean squared error (MSE)					
Individual ANN dedicated for a specific fault type localization	No. of hidden Layers neurons	Network structure	Training performance	Best validation performance	Test performance	Epochs
AG	64	12-16-16-16-16-1	1.65e-5	2.3804e-5	9.6299e-4	1673
BG	64	12-16-16-16-16-1	1.79e-7	6.5471e-5	7.9361e-4	2510
CG	64	12-16-16-16-16-1	8.05e-6	7.1609e-5	3.4148e-4	3000
ABG	72	12-12-12-12-12-24-1	2.82e-7	7.6533e-7	1.2034e-4	2711
ACG	72	12-12-12-12-12-24-1	6.8988e-7	6.9e-7	1.3088e-4	3000
BCG	72	12-12-12-12-12-24-1	7.49e-6	7.491e-6	1.3568e-4	2568
AB	72	12-12-12-12-12-24-1	3.36e-6	3.3646e-6	1.3314e-4	1532
AC	60	12-12-12-12-24-1	1.013e-7	1.2764e-7	1.3713e-4	1223
BC	60	12-12-12-12-24-1	1.727e-6	2.06e-6	2.1987e-4	1610
ABC	72	12-12-12-12-12-24-1	9.2179e-7	1.18e-6	2.148e-4	2121

TABLE VIII. MAIN FEEDER OR LATERALS PREDICTING FAULT LOCATION NEURAL NETS SPECIFICATIONS

Type of ANNs	Cascade forward nets					
Hidden layer transfer function	Tan sigmoid					
Output layer transfer function	Linear					
Training function	Trainlm					
Performance function	Mean squared error (MSE)					
Individual ANN dedicated for a specific fault type localization	No. of hidden neurons	Network structure	Training performance	Best validation performance	Test performance	Epochs
AG	64	12-16-16-16-16-1	3.6082e-5	3.6082e-5	4.1753e-5	3000
BG	64	12-16-16-16-16-1	1.45e-4	5.29e-4	7.77e-4	1524
CG	64	12-16-16-16-16-1	4.3094e-7	6.2e-7	4.3613e-7	3000
ABG	64	12-16-16-16-16-1	7.6533e-7	3.257e-5	1.2034e-4	2350
ACG	64	12-16-16-16-16-1	1.6587e-4	1.66e-4	1.6848e-4	1045
BCG	64	12-16-16-16-16-1	5.208e-4	6.43e-4	5.618e-4	1092
AB	50	12-15-20-15-1	8.3076e-5	8.311e-5	9.1616e-5	2233
AC	64	12-16-16-16-16-1	1.5449e-5	2.2764e-5	3.1259e-5	1416
BC	64	12-16-16-16-16-1	6.32e-11	6.3233e-11	1.0507e-7	3284
ABC	64	12-16-16-16-16-1	1.18e-5	9.2179e-4	1.589e-5	2013

VI. TEST RESULTS AND DISCUSSION

An S-function block with a program written in MATLAB editor environment are used to emulate the

protection scheme built-in functions. The test interval consists of 6 cycles; all the faults are initiated at the beginning of the third cycle. The effect of feeder energization and capacitor switching transients on the protection scheme along with various faults test cases are provided in this section. System condition is declared through an instant message box that contains information of the fault type and location in case of the detection of faults, healthy state declaration in case of no detection of faults.

A. Healthy State Tests

- Capacitor Energization at Node 844

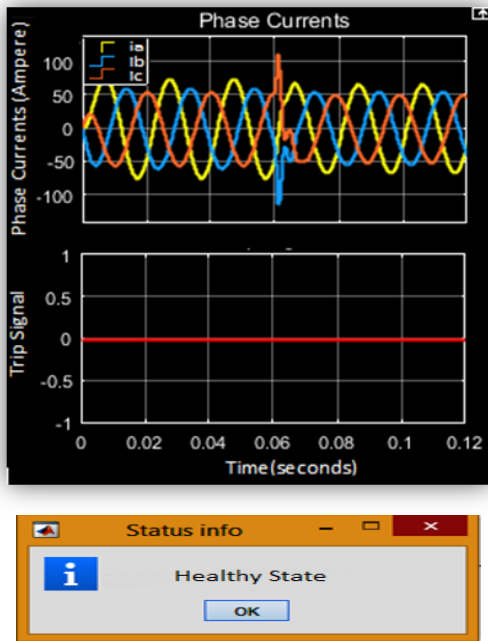


Figure 13. Node 844 Capacitor energization test

- Capacitor Energization at Node 848

B. Faulty State Tests

- Phase A to Ground Fault

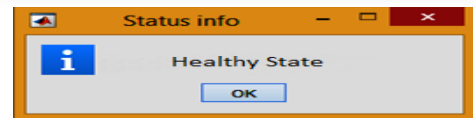
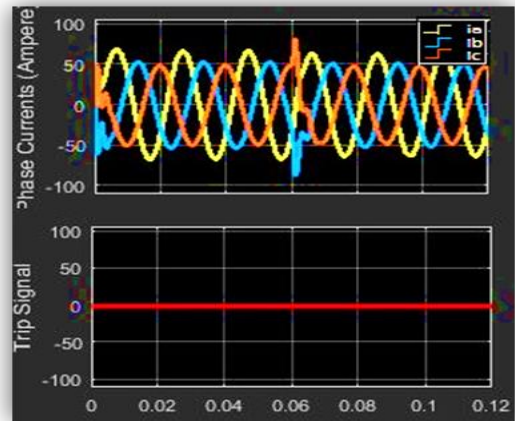


Figure 14. Node 848 capacitor energization test

- Feeder Energization

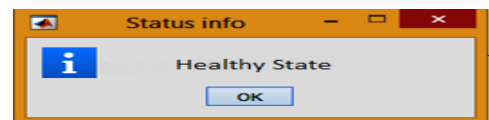
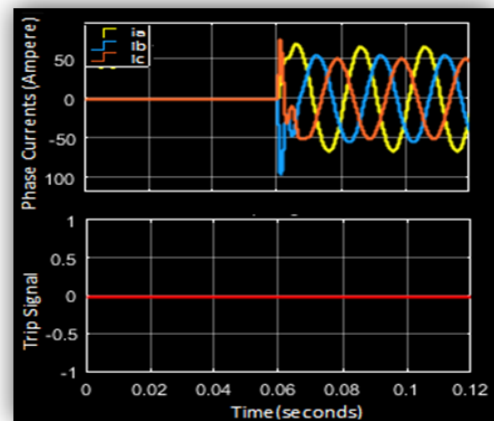
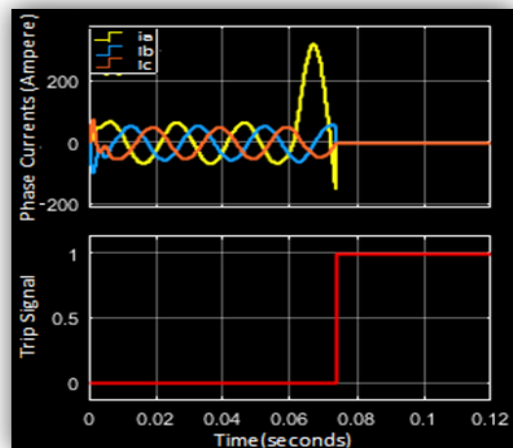


Figure 15. Feeder Energization test



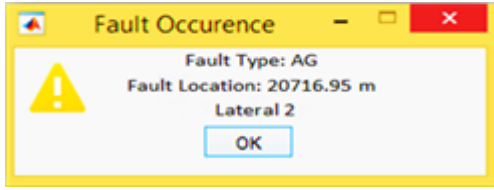


Figure 16. AG fault performed at distance 20727.1 m far from substation and on the lateral 2, the detection of fault is done within 13.805 ms

- Phase B to Ground Fault

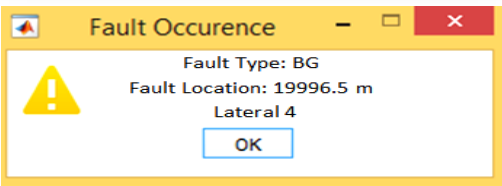
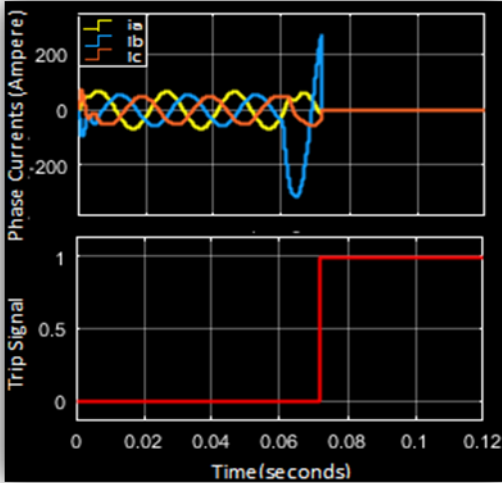


Figure 17. BG fault performed at distance 20000m far from substation and on lateral 4, the detection of fault is done within 11.894 ms

- Phase C to Ground Fault

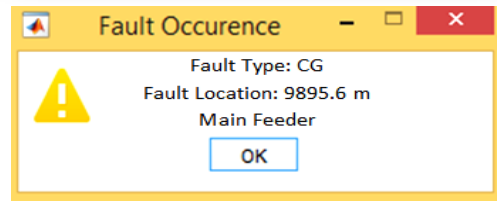
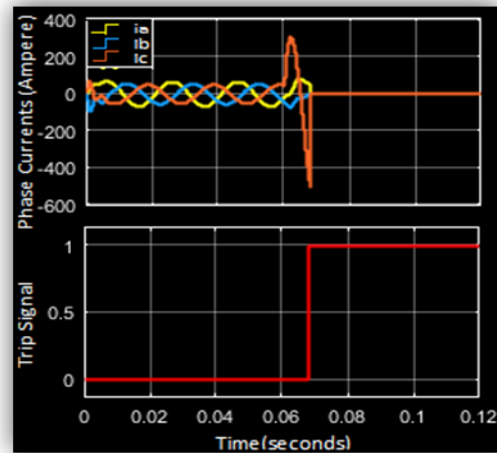


Figure 18. CG fault performed at node 9970 m far from substation on the main feeder, the detection of fault is done within 7.858 ms

- A Double Line Fault Involving Phases A & B to Ground

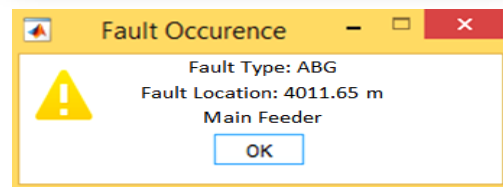
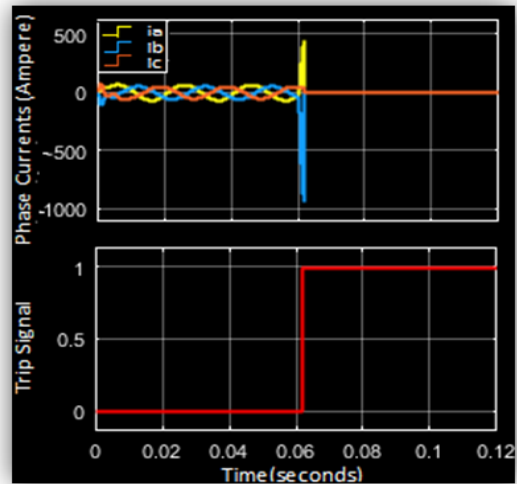


Figure 19. ABG fault performed at 4000 m far from substation on the main feeder, the detection of fault is done within 1.388 ms

- A Double Line Fault Involving Phases A & C to Ground

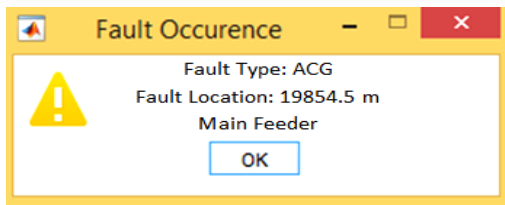
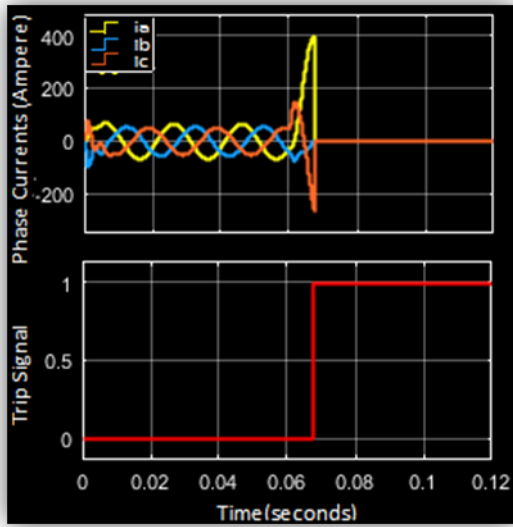


Figure 20. ACG fault performed at distance 20000m far from substation on the main feeder, the fault is detected within 7.117 ms

- A Double Line Fault Involving Phases B & C to Ground

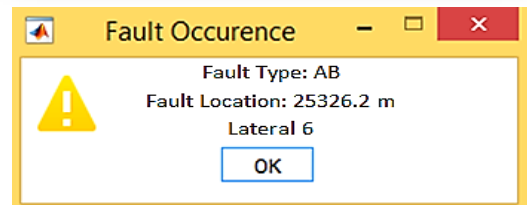
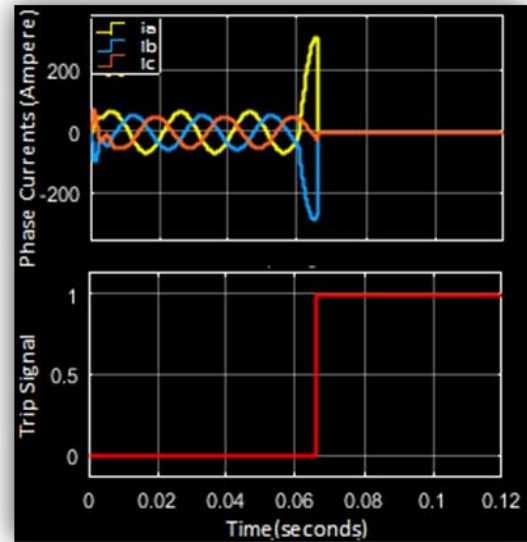


Figure 22. AB fault performed at distance 25478.8 m far from source on lateral 6, the fault is detected within 5.698 ms

- A Double Line Fault Involving Phases A & C

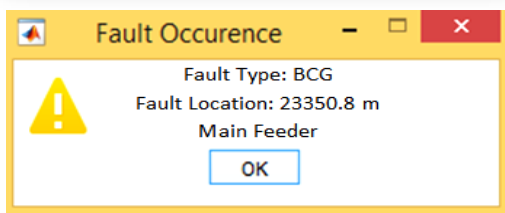
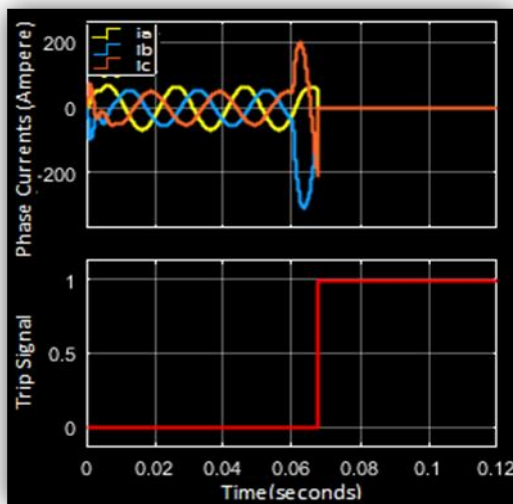


Figure 21. BCG fault performed at 23311 m far from substation on the main feeder, the fault is detected within 7.538 ms

- A Double Line Fault Involving Phases A & B

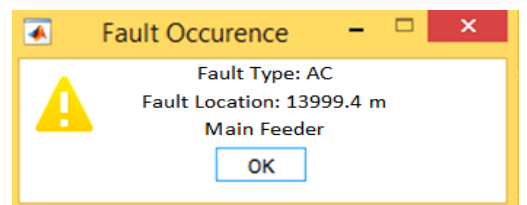
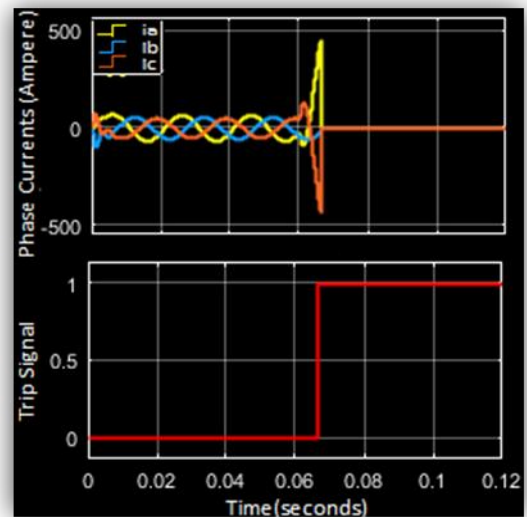


Figure 23. AC fault performed at distance 13970 m far from substation on the main feeder, the fault is detected within 6.163 ms

- A Double Line Fault Involving Phases B & C

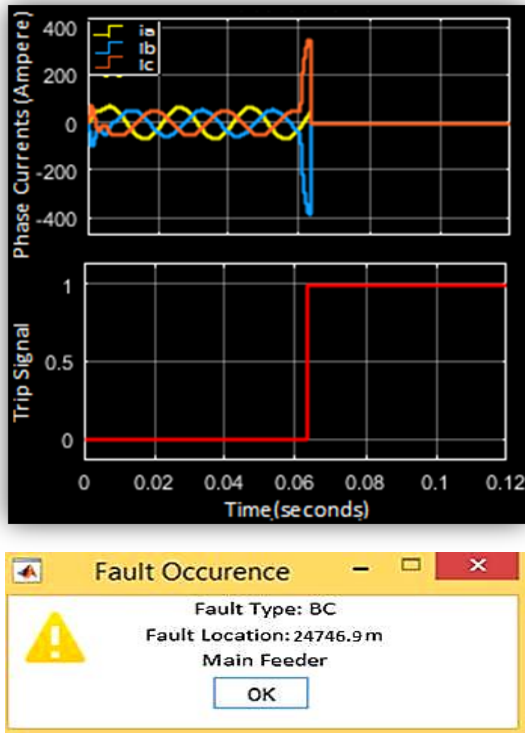


Figure 24. BC fault performed at distance 24863.6 m far from substation on the main feeder, the fault is detected within 3.023 ms

- Three Phase Fault

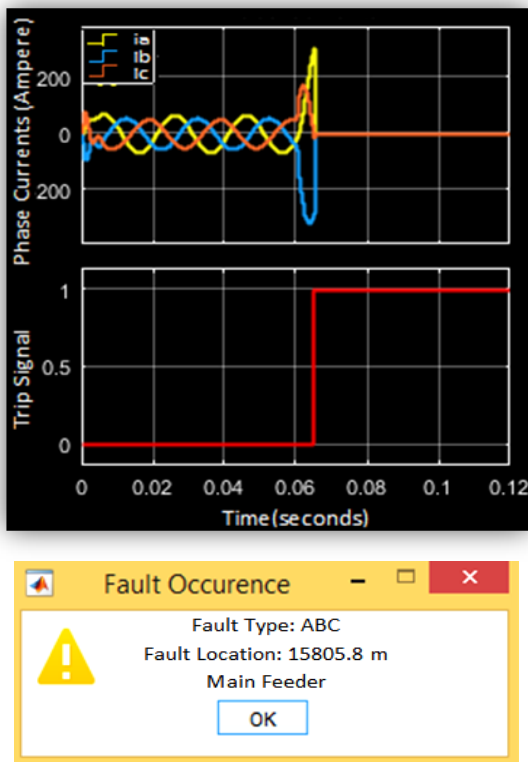


Figure 25. ABC fault performed at 16000 m distant from substation on the main feeder, the fault is detected within 2.907 ms

VII. CONCLUSIONS

The test results of the proposed scheme have shown satisfactory results from the point of view of power system relaying. The first two important characteristics of any protection scheme is that to accomplish the dependability and security during performance. The proposed scheme has proven high dependability in detection such that all tested faults have been investigated properly. The scheme also works securely in a manner that no healthy state has been falsely diagnosed as a faulty state. Another important feature is the ability to diagnose and make a decision in a small amount of time. Response time of the order of few milliseconds is the most preferable in order to isolate and reduce faults severity to humans and power system equipment [33]. With the utilization of the wavelet transform as well as the moving frame technique, major improvements of the speed of fault diagnosis has been experienced.

Obtaining accurate prediction of fault type and location in distribution feeders is a crucial task due to the usual complexity in their structure. Therefore, building a scheme that overcome such complexity is a major requirement in distribution systems protection relaying field. By utilizing the powerful features extraction of the DWT, along with the learning and generalization capabilities of the CFNNs, the task of obtaining useful information about the fault type and location is made possible. The test results show the successful classification and localization of faults without regard to the variation in fault resistances and the presence of structural complexities.

By exploiting the powerful aspects of the proposed protection scheme in protecting distribution feeders, a fast detection of faults can be obtained. Also, a useful information about the faulted phases and the location at which the fault reside can be obtained such that a dispatched maintenance team can find the faulted feeder conductors within less time and effort.

REFERENCES

- [1] M. A. Kafey, "A Wavelet Packet Transform Based on-Line Technique for the Protection of Three-phase Interior Permanent Magnet Motors," M.S. thesis, Memorial University of Newfoundland, St. John's, Canada, May 2006.
- [2] Sonja Ebron, David L. Lubkeman and Mark White, "A neural network approach to the detection of incipient faults on power distribution feeders," *IEEE Transactions on Power Delivery*, vol. 5, pp. 905-912, April 1990.
- [3] Rodrigo Hartstein Salim, Karen Rezende Caino and Arturo Suman Bretas, "Fault detection in primary distribution systems using wavelets," in *Proc. Power Systems Transients Int. Conf.*, France, 2007.
- [4] Omar A. S. Youssef, "Combined fuzzy-logic wavelet-based fault classification technique for power system relaying," *IEEE Transactions on Power Delivery*, vol. 19, pp. 582-589, April 2004.
- [5] Mamta Patel and R. N. Patel, "Fault analysis in transmission lines using neural network and wavelets," in

- Proc. 2015 Signal Processing and Integrated Networks (SPIN) Int. Conf.*, India, 2015, pp. 719-724.
- [6] Majid Jamil, Rajveer Singh, Sanjeev Kumar Sharma, "Fault identification in electrical power distribution system using combined discrete wavelet transform and fuzzy logic," *Journal of Electrical Systems and Information Technology*, Vol. 2, pp. 257-267, September 2015.
- [7] Karen L. Butler and Dr. James A. Momoh, "Detection and classification of line faults on power distribution systems using neural networks," in *Proc. 36th Midwest Symposium on Circuits and Systems*, USA, 1993, pp. 368-371.
- [8] Rameshkumar C. Mishra and P.M. Deoghare, "Analysis of transmission line fault by using wavelet," *International journal of engineering research & technology*, vol. 3, pp. 36-40, May 2014.
- [9] Suman Devi, Nagendra K. Swarnkar, Sheesh Ram Ola and Om Prakash Mahela, "Detection of Transmission Line Faults Using Discrete Wavelet Transform," in *Proc. 2016 Advances in signal processing Conf. (CASP)*, India, 2016, pp. 133-138.
- [10] A. Ngaopitakkul, C. Apisit, C. Pothisarn, C. Jettanasen and S. Jaikhan, "Identification of fault locations in underground distribution system using discrete wavelet transform," in *Proc. 2010 Engineers and Computer Scientists Int. Multi Conf.*, Hong Kong, 2010.
- [11] Liqun Shang, Wensong Zhai and Pei Liu, "Study of Fault Location in Transmission Line Using S Transform," in *Proc. 2016 Computer, Consumer and Control Conf. (IS3C)*, China 2016, pp. 85-88.
- [12] R. Das, M. S. Sachdev and T. S. Sidue, "A Fault Locator for Radial Subtransmission and Distribution Lines," *IEEE Power Engineering Society Summer Meeting*, USA, July 2000, pp. 443-448.
- [13] Rahman Dashti, Mohammad Daisy and Hamid Reza Shaker, "A new Method presentation for locating Fault in Power Distribution Networks," in *Proc. 2016 Electrical Apparatus and Technologies International Symposium (SIELA)*, Bulgaria, June 2016.
- [14] H. Mokhlis and H. Y. Li, "Fault location estimation for distribution system using simulated voltage sags data," in *Proc. 2007 Universities Power Engineering Conf. (UPEC)*, UK, Sept. 2007, pp. 242-247.
- [15] A. H. A. Bakar, M. S. Ali, ChiaKwang Tan, H. Mokhlis and H. Arof, H. A. Illias, "High impedance fault location in 11 kV underground distribution systems using wavelet transforms," *International Journal of Electrical Power & Energy Systems*, vol. 55, pp. 723-730, 2014.
- [16] J. J. Mora, G. Garrillo and L. Pérez, "Fault Location in Power Distribution System using ANFIS Nets and Current Patterns," in *Proc. 2006 Transmission & Distribution Conference and Exposition*, Venezuela, Aug. 2006, pp. 1-6.
- [17] A. Abdollahi and S. Seyedtabaai, "Transmission Line Fault Location Estimation by Fourier & Wavelet Transforms Using ANN," in *Proc. 2010 4th International Power Engineering and Optimization Conference (PEOCO)*, Malaysia, June 2010, pp. 573-578
- [18] Md. Abdul Kalam, Majid Jamil and A. Q. Ansari, "Wavelet based ANN Approach for Fault Location on a Transmission Line," in *Proc. 2010 Power Electronics, Drives and Energy Systems (PEDES) & Power India Joint Int. Conf.*, India, Dec. 2010.
- [19] S. Bunjongjit, A. Ngaopitakkul and C. Pothisarn, "A Discrete Wavelet Transform and Fuzzy Logic Algorithm for Identifying the Location of Fault in Underground Distribution System," in *Proc. 2013 Fuzzy Theory and Its Application (iFUZZY) Int. Conf.*, Taiwan, Dec. 2013, pp. 415-419.
- [20] Kapildev Lout and Raj K. Aggarwal, "A feedforward artificial neural network approach to fault classification and location on a 132kv transmission line using current signals only," in *Proc. 2012 47th Universities Power Engineering Conference (UPEC) Int. Conf.*, UK, Sept. 2012.
- [21] Binoy Saha, Bikash Patel, Parthasarathi Bera, "DWT and BPNN Based Fault Detection, Classification and Estimation of Location of HVAC Transmission Line," in *Proc. 2016 Intelligent Control Power and Instrumentation Int. Conf.*, India, Oct. 2016, pp. 174-178.
- [22] Zhengyou He, Xiaopeng Li, and Shuang Chen, "A travelling wave natural frequency based single ended fault location method with unknown equivalent system impedance," *International Transactions on Electrical Energy Systems*, vol. 26, pp. 509-524, 2016.
- [23] Sunil Singh and D.N. Vishwakarma, "Application of DWT and ANN for fault classification and location in a series compensated transmission line," in *Proc. 2016 IEEE 6th International Conference on Power Systems (ICPS)*, India, March 2016.
- [24] Sadiq I. Hassan, Adil A. Obed, and Khalid M. Abdul-Hassan, "Practical implementation for stator faults Protection and diagnosis in 3-ph IM based on WPT and neural network," *The International Journal of Engineering and Science (IJES)*, vol. 5, pp. 52-67, 2016.
- [25] Martin L. Baughman, Chen-Ching Liu and Roger C. Dugan. (August 2013). IEEE 34 node test feeder. *IEEE PES Power & Energy Society*. [Online]. Available: https://www.ewh.ieee.org/soc/pes/dsacom/testfeeders/feeder_34.zip.
- [26] Q. Fu, A. Solanki, L. F. Montoya, A. Nasiri, V. Bhavaraju, T. Abdallah, D. Yu, "Generation Capacity Design for a Microgrid for Measurable Power Quality Indexes," in *Proc. 2012 IEEE PES Innovative Smart Grid Technologies (ISGT)*, USA, April 2012, pp. 1-6.
- [27] Ndaga Mwakabuta and Arun Sekar, "Comparative Study of the IEEE 34 Node Test Feeder under Practical Simplifications," in *Proc. 2007 39th North American Power Symposium*, USA, Oct. 2007, pp. 484-491.
- [28] Rodrigo Hartstein Salim, Karen Rezende Caino De Oliveira and Arturo Suman Bretas, "Fault detection in primary distribution systems using wavelets," in *Proc. Power Systems Transients Int. Conf.*, France, June 2007.
- [29] F. Martin, J. A. Aguado, M. Medina, and M. Munoz, "Classification of faults in double circuit lines using wavelet transforms," in *proc. 2008 IEEE Int. Conf. on Industrial Technology*, China, Aug. 2008.
- [30] P. K. Kankar, Satish C. Sharma, and S. P. Harsha, "Fault diagnosis of ball bearings using continuous wavelet transform," *Applied Soft Computing*, vol. 11, pp. 2300-2312, 2011.
- [31] Kumar H S, P. Srinivasa Pai, N. S. Sriram, and Vijay Gs, "Selection of mother wavelet for effective wavelet transform of bearing vibration signals," *Advanced Materials Research*, vol. 1039, pp. 169-176, 2014.
- [32] Mark Hudson Beale, Martin T. Hagan and Howard B. Demuth, *Neural Network Toolbox™ User's Guide*, The Math Works Inc., 2016, ch. 3, pp. 1-30.
- [33] S. H. Horowitz, and A. G. Phadke, *Power system relaying*, 3rd Ed., Baldoack, Hertfordshire, England: Wiley, 2008. ch. 1, pp.7-11.